Pergamon

Chemical Engineering Science, Vol. 51, No. 8, pp. 1311–1332, 1996

0009-2509/96 $15.00 + 0.00

0009-2509(95)00299-5

ON THE SOLUTION OF POPULATION BALANCE EQUATIONS BY DISCRETIZATION—I. A FIXED PIVOT TECHNIQUE

SANJEEV KUMAR and D. RAMKRISHNA*
School of Chemical Engineering, Purdue University, West Lafayette, IN 47907, U.S.A.

(*First received* 28 *November* 1994; *revised manuscript received* 21 *March* 1995; *accepted* 9 *July* 1995)

Abstract—A new framework for the discretization of continuous population balance equations (PBEs) is presented in this work. It proposes that the discrete equations for aggregation or breakage processes be internally consistent with regard to the desired moments of the distribution. Based on this framework, a numerical technique has been developed. It considers particle populations in discrete and contiguous size ranges to be concentrated at representative volumes. Particulate events leading to the formation of particle sizes other than the representative sizes are incorporated in the set of discrete equations such that properties corresponding to two moments of interest are exactly preserved. The technique presented here is applicable to binary or multiple breakage, aggregation, simultaneous breakage and aggregation, and can be adapted to predict the desired properties of an evolving size distribution more precisely. Existing approaches employ successively fine grids to improve the accuracy of the numerical results. However, a simple analysis of the aggregation process shows that significant errors are introduced due to steeply varying number densities across a size range. Therefore, a new strategy involving selective refinement of a relatively coarse grid while keeping the number of sections to a minimum, is demonstrated for one particular case. Furthermore, it has been found that the technique is quite general and yields excellent predictions in all cases. This technique is particularly useful for solving a large class of problems involving discrete–continuous PBEs such as polymerization-depolymerization, aerosol dynamics, etc.

1. INTRODUCTION

Beginning with Smoluchowski's description of the stability of mono-dispersed colloids, population balance equations† (PBEs) have found diverse applications in areas involving particulate systems. These equations are particularly useful for situations where particles continually lose their identities, e.g. in crystallizers, liquid–liquid and gas–liquid contactors, microbial fermentors, fluidized beds, polymer reactors (Ramkrishna, 1985). PBEs have also been used to study raindrop size distributions, aerosol dynamics, crushing of materials, stability of emulsions and so on. A successful use of PBEs, however, depends on our ability to solve them numerically as the analytical solutions are rare. The recent thrust on model-based control of particulate systems indicates that, in addition, numerical solutions be accurate and be obtainable in real time.

Several numerical techniques, e.g. method of weighted residuals, method of moments, orthogonal collocation, collocation on finite element, have been proposed in the literature and have been reviewed by Ramkrishna (1985). Computationally, however, the method of discretization of the continuous PBE has emerged as an attractive alternative.

Consider the PBE for a population of particles which undergo break-up as well as aggregation.

$$\frac{\partial n(v,t)}{\partial t} = \tfrac{1}{2}\int_0^v n(v-v',t)n(v',t)Q(v-v',v')\,dv' - \Gamma(v)n(v,t) - \int_0^\infty n(v,t)n(v',t)Q(v,v')dv' + \int_v^\infty \beta(v,v')\Gamma(v')n(v',t)dv'. \quad (1)$$

The moments M_μ of the number density function $n(v,t)$ defined as

$$M_\mu = \int_0^\infty v^\mu n(v,t)\,dv \quad (2)$$

are then obtained from eq. (1) as

$$\frac{dM_\mu}{dt} = -\tfrac{1}{2}\int_0^\infty dv \int_0^\infty dv' [v^\mu + v'^\mu - (v+v')^\mu] \times Q(v,v')n(v,t)n(v',t) + \int_0^\infty dv' n(v',t)\Gamma(v')v'^\mu \times \left[\int_0^{v'} \left(\frac{v}{v'}\right)^\mu \beta(v,v')\,dv - 1\right]. \quad (3)$$

* Corresponding author. Tel.: 317-494-4066. Fax: 317-494-0805. E-mail: ramkrish@ecn.purdue.edu.

† In the physics literature, the PBE for the pure aggregation problem is known as the Smoluchowski equation.

Our interest here is in formulating population balances in discrete particle state space. The quest for a discrete formulation of eq. (1) may be likened to *macroscopic balances* in the analysis of transport problems where one seeks conservation equations for an entity in a chosen finite volume of material or space. Integrating the continuous equation [eq. (1)] over a discrete size interval, say v_i to v_{i+1},

$$\frac{dN_i(t)}{dt} = \frac{1}{2}\int_{v_i}^{v_{i+1}} dv \int_0^v n(v-v', t)n(v', t)Q(v-v', v')dv' - \int_{v_i}^{v_{i+1}} n(v, t)dv \int_0^\infty n(v', t)Q(v, v')dv' + \int_{v^i}^{v_{i+1}} dv \int_v^\infty \beta(v, v')\Gamma(v')n(v', t)dv' - \int_{v_i}^{v_{i+1}} dv\Gamma(v)n(v, t) \quad (4)$$

where

$$N_i(t) = \int_{v_i}^{v_{i+1}} n(v, t)dv. \quad (5)$$

The set of equations (4) reflects a loss of *autonomy*.‡

The basic question here with regard to discretization is whether autonomy can be restored. It will then be possible to solve the discrete equations for the total number of particles in a size range. The accuracy of the numerical solution will of course depend on the manner in which autonomy is restored. The objective of the present paper is therefore to first review the existing literature with regard to this question and then propose a new technique that is general, computationally efficient, and allows improvements in accuracy where needed.

The paper is organized as follows. It begins with a critical assessment of previous work in Section 2. Section 3 deals with the derivation of discrete equations for the new technique. Numerical results are obtained for the cases including polymerization–depolymerization (simultaneous breakup and aggregation) for which analytical solutions exist so that the accuracy of the numerical technique can be reliably evaluated. This is presented in Section 4. Section 5 discusses a major source of error in the numerical solutions and suggests a new approach for improving accuracy. Concluding remarks and summary are presented in the last section.

2. PREVIOUS WORK

A large variety of discretization techniques have been proposed in the literature to solve PBEs. These techniques aim at developing a set of self-contained equations from the set of equations (4) or a slight variation of it. In order to examine these techniques critically, let us first explore eq. (4) in further detail. Assume that the complete size range is divided into smaller size ranges and our interest lies in knowing the events responsible for changes in particle population for the ith size range. This information is contained in eq. (4) and can be represented easily through a graphical procedure, due to Bleck (1970). Figure 1 shows such a representation for all the terms contained on the r.h.s. of eq. (4). Region A represents aggregation events leading to particle formation in the ith size range, as given by the first term; region B indicates death events due to aggregation of particles in the ith size range with other particles including those in the same size range, as given by the second term; region C represents birth events due to the breakup of particles lying in the same or larger size ranges, as expressed by the third term; and region D shows death events due to the breakup of particles in the ith size range, given by the last term in eq. (4). Figure 1 contains some overlapping zones, which indicate that some events contribute to the birth as well as the death of particles from the same size range. These events have been called as intra-interval, whereas the others are known as inter-interval in the existing literature. The figure also shows that for a large discrete size range, intra-interval events can constitute a significant fraction of the total number of events affecting the particle population in it.

An accurate determination of these events clearly requires a knowledge of $n(v, t)$, thus leaving the set of equations (4) unclosed. A closed set of equations can however be obtained by representing the r.h.s. of eq. (4) in terms of N_i's. There are two major approximate approaches to accomplish this: (i) application of the mean value theorem on frequency (to be called the M-I approach) and given as

$$\int_{v_i}^{v_{i+1}} dv \int_{v_k}^{v_{k+1}} dv' n(v, t)n(v', t)Q(v, v') = Q_{i,k}N_i(t)N_k(t), \quad (6)$$

where $Q_{i,k}$ is

$$Q_{i,k} = Q(x_i, x_k); \quad v_i \leqslant x_i \leqslant v_{i+1}, \quad v_k \leqslant x_k \leqslant v_{k+1} \quad (7)$$

and (ii) application of the mean value theorem on number density (to be called the M-II approach) and given as

$$\int_{v_i}^{v_{i+1}} dv \int_{v_k}^{v_{k+1}} dv' n(v, t)n(v', t)Q(v, v') = \bar{n}_i(t)\bar{n}_k(t) \int_{v_i}^{v_{i+1}} dv \int_{v_k}^{v_{k+1}} dv' Q(v, v') \quad (8)$$

where

$$\bar{n}_i(t) = \frac{1}{v_{i+1} - v_i} \int_{v_i}^{v_{i+1}} n(v, t)dv, \quad (9)$$

and the term with a double integral on the r.h.s. of eq. (8) is assumed to be independent of time. Within the broad classification of these two approaches, various

‡ We use the term "autonomy" of a set of equations to express the property of being closed in the set of unknowns (dependent variables).

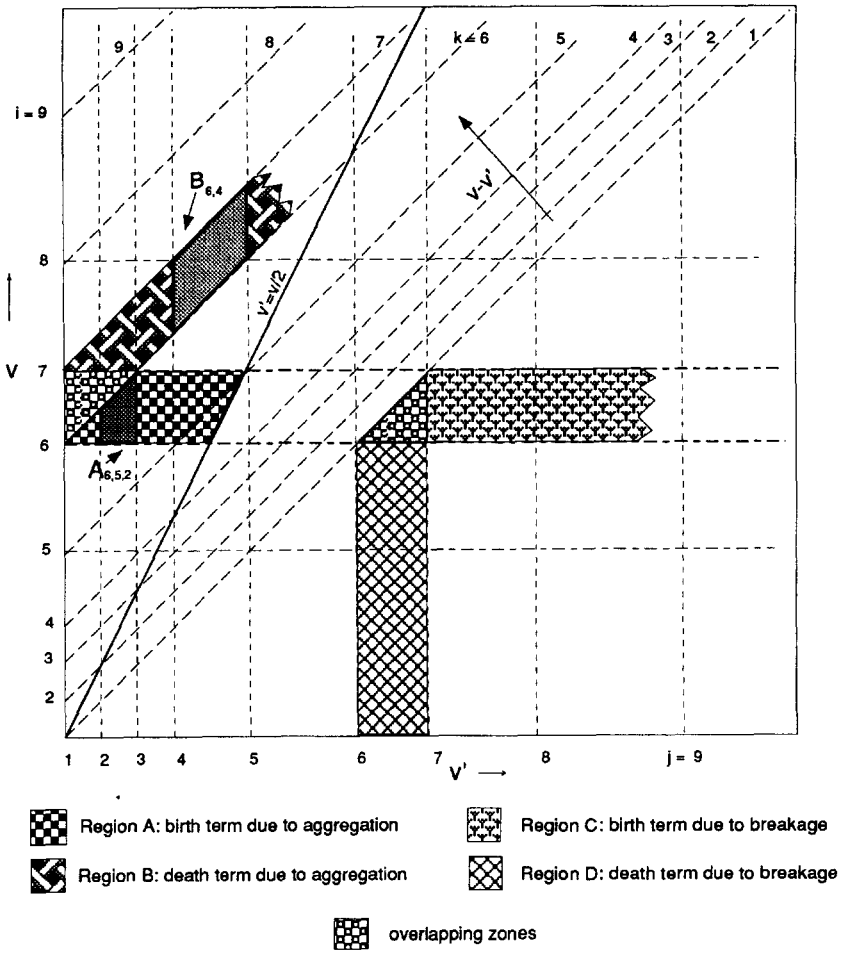

Fig. 1. A graphical representation of birth and death events for a typical size range, as given by eq. (4).

techniques have been proposed in the literature to restore autonomy and are reviewed here in the rest of this section.

Hidy and Brock (1970) used the M-I approach with a linear grid to restore autonomy for PBEs for aggregation alone. They considered particle population in a size range $\{v_i, v_{i+1}\}$ to be represented by size x_i, defined as ix_1. Their final equations are easily obtained by expressing number density as

$$n(v, t) = \sum_{j=1}^{M} N_j \delta(v - x_j) \tag{10}$$

and substituting for it in eq. (4). Thus,

$$\frac{dN_i}{dt} = \frac{1}{2} \sum_{j=1}^{i-1} N_j N_{i-j} Q_{j,i-j} - N_i \sum_{j=1}^{M} N_j Q_{i,j}. \tag{11}$$

The variation of the μth moment can be obtained by substituting for $n(v, t)$ in eq. (3) for aggregation terms alone, which gives

$$\frac{dM_\mu}{dt} = -\frac{1}{2} \sum_{i=1}^{M} \sum_{j=1}^{M} [x_i^\mu + x_j^\mu - (x_i + x_j)^\mu] Q_{i,j} N_i(t) N_j(t). \tag{12}$$

Alternatively, the variation of the μth moment can be obtained by multiplying eq. (11) with x_i^μ and summing it over all i. Thus,

$$\frac{d}{dt}\left(\sum_i N_i x_i^\mu\right) = \frac{dM_\mu}{dt} = -\frac{1}{2} \sum_{i=1}^{M} \sum_{j=1}^{M} [x_i^\mu + x_j^\mu - (x_i + x_j)^\mu] Q_{i,j} N_i(t) N_j(t) \tag{13}$$

Equations (12) and (13) are exactly the same for all values of μ. This indicates that the set of equations (11) can be used to obtain the discrete version of the moments equation for any μ. This of course is a desirable property, and we propose to call it "internal consistency" of the discrete equations with regard to a specific moment, as it ensures that the determination of that particular moment from the size distribution obtained from the solution of the discrete equations is a consistent procedure.

Thus, the discretization technique based on uniform grid yields a set of equations which is internally

values of x_1, the technique provides good resolution at the small size end, and yields extremely accurate solutions for the complete size distribution as well as its moments. The major disadvantage of this technique, though, is that it requires a large number of size ranges to cover the entire size range with acceptable resolution, and therefore incurs very high computational costs.

Batterham *et al.* (1981) used the M-I approach with a geometric grid ($v_{i+1} = 2v_i$) to reduce the number of equations needed to obtain numerical solutions of PBEs for pure aggregation. They considered the particle population in discrete size ranges, $\{v_i, v_{i+1}\}$, to be represented by particle sizes x_i's. The aggregation of these particles led to the formation of new particles lying on the boundaries of a size range. The authors divided such particles equally (mass) between the adjoining size ranges. Also, the particles formed in a subsize range, e.g. x_i to v_{i+1} for the ith size range, were assigned to x_i such that the mass was conserved. Their final equations, which incorporate intra- and interinterval events, are

$$\begin{aligned}\frac{dN_i(t)}{dt} &= (\tfrac{3}{8})N_{i-1}(t)N_{i-2}(t)Q_{i-1,i-2} \\ &\quad + (\tfrac{3}{4})N_i(t)N_{i-1}(t)Q_{i,i-1} \\ &\quad + N_{i-1}(t)N_{i-1}(t)Q_{i-1,i-1} \\ &\quad + \sum_{j=1}^{i-2}(1+2^{j-i})N_j(t)N_i(t)Q_{i,j} \\ &\quad - \sum_{j=1}^{M} N_i(t)N_j(t)Q_{i,j} - N_i(t)N_i(t)Q_{i,i}.\end{aligned} \tag{14}$$

These equations conserve total mass (internal consistency with regard to first moment), but fail to yield the correct discrete equation for total numbers or any other moment [eq. (12)]. Besides these limitations, the authors have counted the aggregation of the equal size particles twice. Koh *et al.* (1987) have used the erroneous equations of Batterham *et al.* (1981), whereas Chen *et al.* (1990) have corrected for the double counting.

Hounslow *et al.* (1988) have proposed a new discretization technique using the M-I approach. They chose the same fixed grid as that of Batterham *et al.* (1981), but assumed the particles to be uniformly distributed in a size range and considered aggregation of particles in fractions of size ranges to form particles in size range $\{v_i, v_{i+1}\}$, also evident from Fig. 1. They identified four types of interactions that can change the total population in a size range and derived expressions for each one of them separately. The set of equations derived thus was internally consistent with respect to only the zeroth moment of the distribution (total numbers) and did not conserve mass. The authors corrected for it by introducing a correction factor, which turns out to be independent of the choice of the aggregation kernel. Their final set of equations is

$$\begin{aligned}\frac{dN_i(t)}{dt} &= N_{i-1}(t)\sum_{j=1}^{i-2}2^{j-i+1}Q_{i-1,j}N_j(t) \\ &\quad + \tfrac{1}{2}Q_{i-1,i-1}N_{i-1}^2(t) \\ &\quad - N_i(t)\sum_{j=1}^{i-1}2^{j-i}Q_{i,j}N_j(t) \\ &\quad - N_i(t)\sum_{j=1}^{M}Q_{i,j}N_j(t),\end{aligned} \tag{15}$$

which is now internally consistent with regard to mass and total numbers. Since these equations cannot result in the correct discrete equation for other moments, it is to be expected that those moments and corresponding densities will not be predicted well (discussed further in Section 4.2.2). The technique is limited to a fixed and coarse geometric grid, and results in poor predictions at long times.

Bleck (1970) seems to have been the first in the literature to suggest a geometric grid for the discretization of PBEs for aggregation. He proposed that if $n(v, t)$ for a size range is taken to be equal to mass average density for the given size range, eq. (4) for aggregation alone can then be exactly reduced to the following by using M-II:

$$\frac{\partial\langle n\rangle_i}{\partial t} = \frac{2}{v_{i+1}^2 - v_i^2}\left(\sum_{j=1}^{i}\sum_{k=1}^{j}a_{ijk}\langle n\rangle_j\langle n\rangle_k - \sum_{k=1}^{M}b_{ik}\langle n\rangle_i\langle n\rangle_k\right). \tag{16}$$

Coefficients a_{ijk} and b_{ik} are given as

$$\begin{aligned}a_{ijk} &= \int\int_{A_{ijk}} Q(\xi, x-\xi)x\,dx\,d\xi, \\ b_{ik} &= \int\int_{B_{i,k}} Q(x,\xi)x\,dx\,d\xi.\end{aligned} \tag{17}$$

Areas A_{ijk} and B_{ik} are shown graphically in Fig. 1. This method of restoring autonomy conserves only mass. The set of equations (16) does not reduce to a correct discrete equation for any other moment. In addition, the technique is computationally more expensive due to the presence of double integrals. For a size-dependent kernel, the numerical results are not in good agreement with the analytical results even for a fine grid ($v_{i+1} = 2^{1/3}v_i$). Nambiar *et al.* (1992) have recently extended Bleck's technique to pure breakup with the same limitations as those in the original technique.

Gelbard *et al.* (1980) have proposed a similar technique for pure aggregation. The authors have derived general conservation equations for property P_i, defined as $\int_{v_i}^{v_{i+1}} v^i n(v, t)\,dv$, by considering various types of aggregation events and then obtaining the corresponding kinetic coefficients. Alternatively, these

equations can be easily derived by discretizing a modified PBE,

$$\frac{\partial p(v,t)}{\partial t} = \tfrac{1}{2}\int_0^v v^\zeta r(v^- v', v') p(v^- v', t) p(v', t)\,\mathrm{d}v' - p(v,t)\int_0^\infty v^\zeta r(v, v') p(v', t)\,\mathrm{d}v' \qquad (18)$$

where $p(v,t) = v^\zeta n(v,t)$ and $r(v,v') = Q(v,v')/v^\zeta v'^\zeta$. The final set of discrete equations can be written as

$$\frac{\partial \langle p\rangle_i}{\partial t} = \frac{1}{v_{i+1} - v_i}\left(\sum_{j=1}^{i}\sum_{k=1}^{j} c_{ijk}\langle p\rangle_j\langle p\rangle_k - \sum_{k=1}^{M} d_{ik}\langle p\rangle_i\langle p\rangle_k\right) \qquad (19)$$

where coefficients c_{ijk} and d_{ik} are given by similar definitions as in eq. (17). The discrete equations of these authors are internally consistent only with regard to the ζth moment. Our predictions using this technique indicate that for $\zeta = 0$, as one would expect, the first moment of the distribution (mass) is not conserved and the results for number density also are not accurate (although the computation time is significantly larger compared to the approaches based on M-I). Sastry and Gaschignard (1981) proposed two sets of equations, one for $\zeta = 0$ and the other for $\zeta = 1$, using the M-II approach. These sets of equations are coupled through the slope of the number density function in the discrete size range. The authors claim their results to be more accurate (although their plots do not extend to the region of eventual exponential decay). Evaluation of a large number of double integrals increases the computational costs significantly.

Landgrebe and Pratsinis (1990) have extended the technique proposed by Gelbard *et al.* (1980) to discretize the discrete–continuous PBE for aggregation, proposed by Gelbard and Seinfeld (1979). They show that, in the limit of a very fine grid, the numerical results remain the same for $\zeta = 0$, 1 or 2. The authors report that for a relatively coarse grid ($v_{i+1} = 1.5v_i$) the best results are obtained with $\zeta = 2$ (which does not preserve other moments), even though as much as 10% mass is lost during the aggregation process.

In a recent paper, Kostoglou and Karabelas (1994) have reviewed various techniques for solving PBEs for pure aggregation. In addition to presenting a general review of various techniques, the authors have tested four techniques for constant and sum kernels. Out of these techniques, the technique proposed by Marchal *et al.* (1988), which is based on M-I, does not preserve numbers and gives the worst performance. The technique proposed by Gelbard *et al.* (1980), reviewed earlier in this section, offers the next best performance. Surprisingly, the technique proposed by Batterham *et al.* (1981) (also reviewed earlier), which does not preserve numbers and counts the aggregation of the particles in the same size range twice, yields nearly as good a performance as the best choice, the technique proposed by Hounslow *et al.* (1988). This appears to be due to the cancellation of errors. In a new situation, cancellation of errors may not always be guaranteed.

From the foregoing survey of the use of discretization methods, the following conclusions emerge: (i) Techniques based on M-I have the merit of computational efficiency. (ii) Finer grids improve accuracy of the solution. (iii) Procedures conserving *both* particle numbers and mass also improve accuracy.

This paper presents an approach that substantially improves the effectiveness of discretization methods in various ways. First, it leaves open any two properties for exact preservation during aggregation or breakage depending on what moments of the population are desired accurately. Second, the coarseness of discretization may be varied depending on the distribution of the errors in number density. This ability to vary the discretization can be naturally exploited to deal with discrete–continuous formulations of population balance. For example, in polymerization, the smaller polymers are purely discrete (in chain length) requiring a uniform discretization and the larger polymers may be approximated by continuous chain lengths requiring a suitably coarse discretization different from that of the smaller entities. Third, the method is free from *ad hoc* derivations and accommodates naturally diverse combinations of aggregation and breakage events.

3. FORMULATON OF DISCRETE EQUATIONS

Often the quantity of engineering interest is some integral property associated with the entire population that can be calculated as the sum of those attributed to individual particles. Consider, for example, property $F(t)$ for the entire population, calculable from property $f(x)$ of a single particle of volume x. The total property $F(t)$ can then be obtained as

$$F(t) = \int_0^\infty f(x) n(x,t)\,\mathrm{d}x. \qquad (20)$$

Suppose further that the application concerned requires the precise evolution of $F(t)$. Equation (20) shows that the most accurate way to calculate the evolution of property $F(t)$ is to obtain the evolution of number density, $n(x,t)$, which can also be used to obtain any other integral property. It is here that the techniques of the present paper become important. Our discrete formulation, instead, directly addresses how changes in certain desired properties $F_1(t)$, $F_2(t)$, $F_3(t)$, ... are brought about by enforcing exact preservation of changes in properties $f_1(x), f_2(x), f_3(x), \ldots$, when particles break or aggregate with other particles. In other words, the discrete equations are designed to produce the "correct" equation for the evolution of $F(t)$. While earlier considerations were limited to total numbers and mass, the considerations here clearly represent generalizations. Although such generalizations may be obvious, it may not be as apparent that the attempt here is to focus on the most

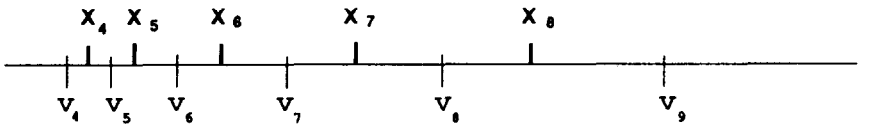

Fig. 2. A general grid which can be used with the proposed numerical technique. Here, $v_i = (x_{i-1} + x_i)/2$.

relevant calculations, i.e. estimation of $F_1(t)$, $F_2(t)$, $F_3(t)$, ... without resorting to the "overkill" of accurately estimating the original number density function or any other (less relevant) property derived from it. Discretization, particularly in its coarse version, is a conscious approximation which, in stressing accuracy on some properties in the interest of the application, *must* necessarily relax on others.

The foregoing discussion focuses on the applications that require the evolution of some integral properties for the entire population. There are other applications where, in addition to integral properties, accurate information is also needed on how these properties are distributed in the particle volume space. This may best be obtained through number density, $n(x, t)$, as the relevant distribution functions, $[f_1(x)n(x, t)]$, $[f_2(x)n(x, t)]$, ..., can now be calculated. The prediction of $n(x, t)$ is computation intensive. Moreover, the estimates of $n(x, t)$ in the size range that contributes substantially to an integral property (e.g. higher moments) will have to be very accurate, although for total numbers such accuracies in $n(x, t)$ may be meaningless and also very difficult to obtain. In most applications, we, however, require only total estimates of these properties for various size ranges of interest (i.e. total number of particles in each section), and it is for such applications that the techniques of the present paper again become important. Our discrete formulation alleviates the problem of estimating $n(x, t)$ very accurately for higher moments by directly addressing the evolution of $F_{i,k}(t)$, total $f_i(x)$ property for section k, through exact preservation of changes in these properties, when the particles break up and aggregate. As pointed out earlier, the formulation stresses on accurate estimation of the quantities of interest while relaxing on other less needed quantities. The idea here is to pick out accurate solutions for the quantities of interest without having to solve for the complete number density (which contains more information than needed).

It may appear that the total integral property can be predicted accurately only if its distribution in particle volume space is also predicted accurately. This is not true as many distributions can correspond to the same integral property. A coarse discretization yields good results for the integral property, even though the distribution of this property may be in small error with the actual distribution. An accurate prediction of the distribution of integral properties thus calls for a flexible technique that can be used with a variety of grids: coarse or fine; uniform, geometric or nonregular (arbitrary).

The numerical technique proposed here divides the entire size range into small sections. The size range contained between two sizes v_i and v_{i+1} is called the ith section. The particle population in this size range is represented by a size x_i (also called grid point), such that $v_i < x_i < v_{i+1}$. A typical grid along with its representative volumes (grid points) is shown in Fig. 2. Unlike the grids proposed in the past, which are either uniform or a fixed geometric type ($v_{i+1} = 2v_i$), the grid proposed here can not only be of geometric type with varying coarseness, but it can also have a more general and flexible pattern, fine in some size ranges and coarse elsewhere. Such grids are later shown to be quite useful for improving the accuracy and also adapting to special situations, e.g. solution of discrete–continuous PBEs for polymerization–depolymerization and other similar problems. The method of restoring autonomy is based on M-I as it does not require the evaluation of any double integrals and is computationally very efficient.

3.1. *Representation of breakup and aggregation events*

The focus of the present technique is a nonuniform grid, as it allows a large size range to be covered with a small number of sections and yet offers good resolution. Since the particle populations in various size ranges are assumed to exist only at corresponding representative sizes, aggregation or breakage of particles of these sizes can result in the formation of new particles whose sizes do not match with any of the representative sizes. Such particles need to be represented through the chosen representative sizes, for which there are a variety of ways, however.

Let us, for example, consider aggregation of two particles of sizes x_j and x_k. In general, aggregation can be defined as change in property $f(x)$ from $f(x_j) + f(x_k)$ to $f(x_j + x_k)$, where $f(x)$ is an extensive property, obtainable from x, the size of a particle. In the framework of purely discrete populations and uniform grid ($x_i = ix_1$), the size of a new aggregate always exactly matches with one of the x_i's. Thus, for this discretization, changes in any property $f(x)$ corresponding to the aggregation of two particles are exactly preserved.

If the changes in an arbitrary property $f(x)$, due to aggregation of particles, are exactly preserved in the representation of these events in the equations for $N_i(t)$'s, it can be shown that the set of equations for $N_i(t)$'s then remains internally consistent with regard to the corresponding property $F(t)$ [eq. (20)] of the size distribution. It is for this reason that the uniform

discretization provides internal consistency with regard to all the moments, as noted in Section 2.

If the size of the new particle does not match with any of the representative sizes, many possibilities exist with regard to its representation. We propose that, instead of an *ad hoc* representation, the particle should be assigned to the nearby representative sizes such that the changes in properties $f_1(x)$, $f_2(x), f_3(x)$, ... due to aggregation or breakage events are exactly preserved in equations for $N_i(t)$'s. The final set of equations for $N_i(t)$'s will then yield the correct discrete equations for the evolution of $F_1(t)$, $F_2(t), F_3(t)$, ... and will allow their prediction from the size distribution in a consistent manner.

For the purpose of illustration, let us consider an example where our interest is in predicting the evolution of the second moment of the distribution. Imagine that a particle of size v $(x_i < v < x_{i+1})$ is formed due to breakage or aggregation of other particles. As stated earlier, to predict the second moment of the distribution in a consistent manner, this particle of size v should be represented through populations at sizes x_i or/and x_{i+1} in such a way that the change in the corresponding property for the second moment, which is $v^2 - x_j^2 - x_k^2$, is exactly preserved. More simply, the reassigned particles should have second moment equal to v^2. Formation of $(v/x_i)^2$ particles of size x_i or $(v/x_{i+1})^2$ particles of size x_{i+1}, both preserve the desired property. Clearly, at least one more property should be preserved to uniquely specify an aggregation or breakage event. In the present work, therefore, we will provide for the exact preservation of two properties, the minimum required.

Yet another point that needs clarification before formulation of the discrete equations is undertaken concerns intra- and inter-interval events. Unlike previous works, in the present paper, distinction between the two types of events is unnecessary for the following reasons. First, all possible events that lead to the formation of new particles in a discrete size range will be considered as birth terms. Second, all possible events that lead to the loss of a particle from a given population will be considered as loss terms. Thus, the intra-interval events that result in the birth as well as the loss of particles from the same size range will be considered twice, but they will be treated like inter-interval events eliminating the need for special considerations for intra-interval events. This simplifies the derivation as well as the implementation of the discrete equations quite substantially.

3.2. *Strategy for conserving two properties*

When a new particle, formed either due to breakup or aggregation, has its size corresponding to a representative size, all the properties associated with it are naturally preserved. However, when such a situation does not exist, we propose that the particle be assigned to the adjoining representative volumes such that two prechosen properties of interest are exactly preserved. Thus, the formation of a particle of size v in size range $\{x_i, x_{i+1}\}$, due to breakup or aggregation, is represented by assigning fractions $a(v, x_i)$ and $b(v, x_{i+1})$ to particle populations at x_i and x_{i+1}, respectively. For the conservation of two general properties $f_1(v)$ and $f_2(v)$, these fractions satisfy the following equations:

$$\begin{aligned} a(v, x_i)f_1(x_i) + b(v, x_{i+1})f_1(x_{i+1}) &= f_1(v) \\ a(v, x_i)f_2(x_i) + b(v, x_{i+1})f_2(x_{i+1}) &= f_2(v). \end{aligned} \tag{21}$$

Although these equations can be generalized for the preservation of four properties by assigning a particle of size v to populations at x_{i-1}, x_i, x_{i+1} and x_{i+2}, in the present paper, we will focus on exact preservation of only two power-law properties, x^ζ and x^ν.

It is clear from these equations that for preservation of two properties, the particle population at x_i gets net particles assigned to it for every new particle that is born in the size range $\{x_{i-1}, x_{i+1}\}$. Using this simple technique for handling new particles, we will now derive discrete equations for breakage and aggregation.

3.3. *Breakage*

Birth term: In the light of the discussion presented in the previous section, the birth term due to particle breakage [third term on the r.h.s. of eq. (4)] given by

$$R_{Bb} = \int_{v_i}^{v_{i+1}} \mathrm{d}v \int_v^\infty \beta(v, v')\Gamma(v')n(v', t)\mathrm{d}v' \tag{22}$$

is modified to

$$\begin{aligned} R_{Bb} = &\int_{x_i}^{x_{i+1}} a(v, x_i)\mathrm{d}v \int_v^\infty \beta(v, v')\Gamma(v')n(v')\,\mathrm{d}v' \\ &+ \int_{x_{i-1}}^{x_i} b(v, x_i)\mathrm{d}v \int_v^\infty \beta(v, v')\Gamma(v')n(v')\,\mathrm{d}v'. \end{aligned} \tag{23}$$

Since the particle population is assumed to be concentrated at representative sizes, x_i's, the number density $n(v, t)$ can be expressed as

$$n(v, t) = \sum_{k=1}^{M} N_k(t)\delta(v - x_k). \tag{24}$$

Substituting for $n(v, t)$ from eq. (24) in eq. (23), we obtain

$$\begin{aligned} R_{Bb} = &\sum_{k \geqslant i} \Gamma_k N_k(t) \int_{x_i}^{x_{i+1}} a(v, x_i)\beta(v, x_k)\mathrm{d}v \\ &+ \sum_{k \geqslant i} \Gamma_k N_k \int_{x_{i-1}}^{x_i} b(v, x_i)\beta(v, x_k)\mathrm{d}v. \end{aligned} \tag{25}$$

Substitution of $a(v, x_i)$ and $b(v, x_i)$ from solutions of sets of equations similar to that in eq. (21) simplifies eq. (25) to

$$R_{Bb} = \sum_{k=i}^{M} n_{i,k}\Gamma_k N_k(t). \tag{26}$$

Here, Γ_k is $\Gamma(x_k)$ and $n_{i,k}$, interpreted as the contribution to population at ith representative size due to the breakage of a particle of size x_k, is given as

$$n_{i,k} = \frac{B_{i,k}^{(\zeta)} x_{i+1}^{\nu} - B_{i,k}^{(\nu)} x_{i+1}^{\zeta}}{x_i^{\zeta} x_{i+1}^{\nu} - x_i^{\nu} x_{i+1}^{\zeta}} + \frac{B_{i-1,k}^{(\zeta)} x_{i-1}^{\nu} - B_{i-1,k}^{(\nu)} x_{i-1}^{\zeta}}{x_i^{\zeta} x_{i-1}^{\nu} - x_i^{\nu} x_{i-1}^{\zeta}} \tag{27}$$

where $B_{i,k}^{(\xi)}$ is given as

$$B_{i,k}^{(\xi)} = \int_{x_i}^{x_{i+1}} v^{\xi} \beta(v, x_k) \mathrm{d}v. \tag{28}$$

The exact preservation of numbers and mass is achieved by setting $\zeta = 0$, $\nu = 1$. For such a case, $n_{i,k}$ is given by a simple form,

$$n_{i,k} = \int_{x_i}^{x_{i+1}} \frac{x_{i+1} - v}{x_{i+1} - x_i} \beta(v, x_k) \mathrm{d}v + \int_{x_{i-1}}^{x_i} \frac{v - x_{i-1}}{x_i - x_{i-1}} \beta(v, x_k) \mathrm{d}v. \tag{29}$$

The first and second integral terms reduce to zero for $i = k$ and $i = 1$, respectively. The integral terms appearing in eqs (28) or (29) can be evaluated analytically for a large class of $\beta(v, v')$ functions. Otherwise, these one-dimensional integrals can be evaluated numerically at negligible computational cost.

Death term: Substituting for $n(v, t)$ from eq. (24) in the death term [last term in eq. (4)] given by

$$R_{Db} = \int_{v_i}^{v_{i+1}} \Gamma(v) n(v, t) \mathrm{d}v \tag{30}$$

we obtain

$$R_{Db} = \Gamma_i N_i(t). \tag{31}$$

3.3.1. *Discrete equations for the pure breakup process.* Substitution of eqs (26) and (31) in eq. (4) for terms corresponding to breakup alone results in the discretized version of PBE for pure breakup, and is given as

$$\frac{\mathrm{d}N_i(t)}{\mathrm{d}t} = \sum_{k=i}^{M} n_{i,k} \Gamma_k N_k(t) - \Gamma_i N_i(t). \tag{32}$$

The set of equations (32) and the accompanying derivation indicate that the technique presented here is free from the form of the breakage function and also the choice of the grid. This allows a single technique to be used for binary, multiple or even the type of breakage proposed by Narsimhan *et al.* (1980) which allows for the formation of more daughter particles as the size of the parent particle increases.

The final equations, obtained here, satisfy the well-known constraints too, e.g., for $\zeta = 0$, $\nu = 1$ and $x_1 = 0$, the following constraints are exactly satisfied.

$$\int_0^{x_k} \beta(v, x_k) \mathrm{d}v = \gamma(x_k)$$
$$\int_0^{x_k} v \beta(v, x_k) \mathrm{d}v = x_k. \tag{33}$$

Here, $\gamma(x_k)$ is the average number of daughter particles formed due to the breakage of a particle of size x_k. For other values of ζ and ν, similar constraints about higher moments are exactly satisfied.

3.4. *Aggregation*

Birth term: Similar to the birth term due to breakage, the birth term due to aggregation [first term on the r.h.s. of eq. (4)] given by

$$R_{Ba} = \tfrac{1}{2} \int_{v_i}^{v_{i+1}} \mathrm{d}v \int_0^v n(v - v', t) n(v', t) Q(v - v', v') \mathrm{d}v' \tag{34}$$

is also modified. The population at representative volume x_i gets a fractional particle for every particle that is born in size range (x_i, x_{i+1}) or (x_{i-1}, x_i). For particles born in range (x_i, x_{i+1}), $a(v, x_i)$ particles are assigned to x_i, and for those born in range (x_{i-1}, x_i), $b(v, x_i)$ particles are assigned. The values of $a(v, x_i)$ and $b(v, x_i)$ are given by the solutions of equations similar to those in eqs (21). Thus, the aggregation term R_{Ab} is modified to

$$R_{Ab} = \tfrac{1}{2} \int_{x_i}^{x_{i+1}} a(v, x_i) \mathrm{d}v \int_0^v n(v - v', t) n(v', t) \times Q(v - v', v') \mathrm{d}v' + \tfrac{1}{2} \int_{x_{i-1}}^{x_i} b(v, x_i) \mathrm{d}v \int_0^v n(v - v', t) n(v', t) \times Q(v - v', v') \mathrm{d}v'. \tag{35}$$

Substituting for $n(v, t)$ from eq. (24), and after some algebraic manipulations, we obtain

$$R_{Ab} = \sum_{\substack{j,k \\ x_{i-1} \leqslant (x_j + x_k) \leqslant x_{i+1}}}^{j \geqslant k} (1 - \tfrac{1}{2} \delta_{j,k}) \eta Q_{j,k} N_j(t) N_k(t) \tag{36}$$

where

$$\eta = \begin{cases} \dfrac{v^{\zeta} x_{i+1}^{\nu} - v^{\nu} x_{i+1}^{\zeta}}{x_i^{\zeta} x_{i+1}^{\nu} - x_i^{\nu} x_{i+1}^{\zeta}}, & x_i \leqslant v \leqslant x_{i+1} \\ \dfrac{v^{\zeta} x_{i-1}^{\nu} - v^{\nu} x_{i-1}^{\zeta}}{x_i^{\zeta} x_{i-1}^{\nu} - x_i^{\nu} x_{i-1}^{\zeta}}, & x_{i-1} \leqslant v \leqslant x_i \end{cases} \tag{37}$$

and

$$Q_{j,k} = Q(x_j, x_k). \tag{38}$$

For preservation of numbers and mass, η is given by the simple expressions

$$\eta = \begin{cases} \dfrac{x_{i+1} - v}{x_{i+1} - x_i}, & x_i \leqslant v \leqslant x_{i+1} \\ \dfrac{v - x_{i-1}}{x_i - x_{i-1}}, & x_{i-1} \leqslant v \leqslant x_i. \end{cases} \tag{39}$$

Equation (36) applies for a general grid. Possible combinations of classes j and k satisfying the consraint $x_{i-1} \leqslant (x_j + x_k) \leqslant x_{i+1}$ are determined at the time of grid generation, which eliminates the need for checking the same inequalities in eq. (37) repeatedly as the computation proceeds.

Loss term: Substituting for $n(v, t)$ from eq. (24) in the death term [fourth term on the r.h.s. of eq. (4)] given by

$$R_{Da} = \int_{v_i}^{v_{i+1}} n(v, t)\mathrm{d}v \int_0^{\infty} n(v', t)Q(v, v')\mathrm{d}v', \quad (40)$$

we obtain

$$R_{Da} = N_i(t) \sum_{k=1}^{M} Q_{i,k}N_k(t). \quad (41)$$

3.4.1. *Discrete equations for the pure aggregation process.* The discrete equations for pure aggregation are obtained by substituting for the birth and the loss terms from eqs (36) and (41) in eq. (4) for aggregation terms alone. The final set of discrete equations is given as

$$\frac{\mathrm{d}N_i(t)}{\mathrm{d}t} = \sum_{\substack{j,k \\ x_{i-1} \leqslant (x_j + x_k) \leqslant x_{i+1}}}^{j \geqslant k} (1 - \tfrac{1}{2}\delta_{j,k})\eta Q_{j,k}N_j(t)N_k(t) - N_i(t) \sum_{k=1}^{M} Q_{i,k}N_k(t). \quad (42)$$

The set of equations (42), like that for pure breakage, has been derived without any reference to the form of the aggregation kernel and the pattern of the grid, thus indicating that these equations are valid for various choices of the aggregation kernel and different grid patterns.

The final equations obtained here offer interesting comparisons with the earlier techniques, reviewed in detail in Section 2. For a geometric grid ($x_{i+1} = 2x_i$) and $\zeta = 0$, $\nu = 1$, the set of equations (42) reduces exactly to that given by Hounslow *et al.* (1988), who derived their equations by following an entirely different set of arguments. Although the final equations are the same, the present technique offers numerous advantages. Derivation of the final equations is quite simple. The technique can be used with a finer geometric grid of type $x_{i+1} = sx_i$, $s > 1$, or other complex grids, e.g. the one shown in Fig. 2, without requiring a new derivation. Most importantly, it can preserve any two properties, not just mass and numbers. Later in Section 4.2.2, we will show that this has important implications. The set of equations in (42) also reduces to the set of discrete equations proposed by Hidy (1965) for uniform discretization, and possesses internal consistency with regard to all the properties. In comparison with the technique proposed by Bleck (1970), which conserves only mass, and by Gelbard *et al.* (1980), which preserves only one property, the present technique preserves two properties and is computationally more efficient as no double integrals need to be evaluated.

An interesting application of an arbitrary grid, that the present technique offers, concerns the discretization of a discrete–continuous PBE proposed by Gelbard and Seinfeld (1979). Landgrebe and Pratsinis (1990) discretized this equation using a lengthy and involved derivation with double integrals and conservation of only one property. In comparison, the present technique, with a uniform grid at small size range and a geometric grid at large size range, addresses several important issues with the discrete–continuous PBE quite easily. A uniform grid at small sizes naturally reduces to purely discrete populations here and a geometric grid covers a long size range with a small number of equations, preserves two properties of the distribution, allows improvement in accuracy through manipulation of the grid and requires only reduced computational effort.

3.5. *Discretized equations for simultaneous breakup and aggregation*

The discretization techniques used for breakage and aggregation are based on a common strategy and involve the same variables $N_i(t)$'s, thereby allowing us to combine discrete equations for breakage and aggregation in a straightforward way to obtain discrete equations for simultaneous breakage and aggregation. The final equations are

$$\frac{\mathrm{d}N_i(t)}{\mathrm{d}t} = \sum_{\substack{j,k \\ x_{i-1} \leqslant (x_j + x_k) \leqslant x_{i+1}}}^{j \geqslant k} (1 - \tfrac{1}{2}\delta_{j,k})\eta Q_{j,k}N_j(t)N_k(t) - N_i(t) \sum_{k=1}^{M} Q_{i,k}N_k(t) + \sum_{k=i}^{M} n_{i,k}\Gamma_k N_k(t) - \Gamma_i N_i(t). \quad (43)$$

The set of equations (43) has quite general applicability. Like the previous sets of equations for pure breakage and pure aggregation, these equations are valid for various functional forms for the breakage frequency, daughter particle size distribution function and aggregation kernel. If properties x^{ζ} and x^{ν} are preserved in the derivation of the discrete equations for both breakage and aggregation terms, the final equations will be internally consistent with regard to the ζth and νth moments of the size distribution. This enables their determination in a consistent manner. Thus, depending on the quantities of interest, the discretization technique can be adapted to yield improved results for the desired quantities.

The use of a numerical technique is called for only when analytical solutions are not available. However, the numerical solutions need to be checked for convergence and accuracy before they can be accepted. This is easily accomplished by comparing the numerical results for two grids that differ only slightly. A numerical technique that uses a fixed grid (Hounslow *et al.*, 1988) cannot be used for this purpose. In comparison, the present technique permits variations in the grid, thereby allowing the convergence and the accuracy of the numerical solutions to be tested easily.

4. NUMERICAL RESULTS

4.1. *Pure breakage*

We consider two examples to illustrate the usefulness of the technique developed here, uniform binary

breakup and multiple breakup. Let us set the quantities of interest to be the integral property total number of particles and its distribution in terms of total numbers in various size ranges along with total mass conservation. Thus, the choice of parameters reduces to $\zeta = 0$ and $\nu = 1$. The complete analytical solutions for the evolution of number density for these cases have been provided by Ziff and McGrady (1985) and Ziff (1991), respectively. All the numerical results presented in this section have been obtained for a geometric grid ($x_{i+1} = sx_i$) and a monodispersed initial condition.

Figure 3(a) shows a comparison of the numerical and the analytical solutions for the variation of total number of particles for $\beta(v, v') = 2/v'$ and $\Gamma(v) = v^2$. The figure shows that the predictions for $N(t)/N(0)$ are in very good agreement with the analytical results, even though a very coarse grid ($s = 3$) has been used here.

The corresponding predictions for size distributions are shown in Fig. 3(b). Before we can compare these results with the analytical solutions, an explanation of the method of comparison is in order. As seen from the previous section, the present technique yields particle populations for various sections at their respective representative volumes. Since the section widths change with the type of grid used, a common basis for comparing the numerical and the analytical results has been provided through a comparison of the average densities. These densities have been plotted at representative volumes or grid points (projection of all the points for a simulation on abscissa indicates the type of grid used to obtain those results). The average number densities for the analytical solutions have been obtained for the finest grids as they are rather insensitive to the type of grid chosen. This strategy of comparing the numerical results has been followed throughout this work. We now go back to Fig. 3(b), which shows the numerical results for the complete size distributions for $s = 2$ and 3, along with the analytical results. The figure shows that the numerical results for $s = 3$ are in good agreement with the analytical results for small as well as very large values of $N(t)/N(0)$ (~ 300) and as the grid is made finer ($s = 2$), the accuracy is further improved. It should be noted that the results have been compared on a log–log plot and the agreement such as the one shown here across many orders of magnitude is indeed remarkable.

A similar exercise has been carried out for multiple breakage. We have added to the level of difficulty here by choosing a situation where 33 daughter particles are produced due to the breakage of a single parent particle and number density approaches infinity as $v \to 0$. Figures 4(a) and 4(b) show that even for this case, the total numbers as well as the complete size distributions are predicted very well for both short and long times. It should be noted that in this case, numerical results have been obtained by using even coarser grids ($s = 3$ and 4). Both of these examples illustrate that pure breakup problems can be handled very well by the present technique, without even requiring a fine grid.

4.2. *Pure aggregation*

4.2.1. *Complete size distribution.* Scott (1968) has presented analytical solutions for pure aggregation for three kernels (constant, sum and product) and various initial conditions. We have compared our numerical results with the analytical solutions for all the three kernels, and for the following initial condition:

$$n(v, 0) = \frac{N_0}{v_0}\left(\frac{v}{v_0}\right)\exp\left(\frac{-v}{v_0}\right). \tag{44}$$

The numerical results have been obtained for the preservation of $\zeta = 0$ (numbers) and $\nu = 1$ (mass) using geometric grids for three values of parameter s. The size of the smallest particle considered here is 2000 times smaller than the initial average particle size. The number of particles and the fractional mass contained in particles smaller than this size is insignificant and does not change the numerical results. The method of comparison here is the same as that used in the previous section. For $\zeta = 0$, $\nu = 1$ and $s = 2$, as pointed out in Section 3.4, our equations become identical to those of Hounslow *et al.* (1988); therefore, the other results for smaller values of parameter s can be viewed as improvements over the results obtained by the technique proposed by Hounslow *et al.* (1988).

Figure 5 shows the complete size distributions for the constant kernel at two degrees of aggregation [defined as $N(t)/N(0)$], and for three selections of grid parameter s (2, 1.5 and 1.25). The results have been plotted using a log–log scale to highlight the deviations from the analytical results in the size range where the number density decreases steeply. The use of a linear scale does not show such differences. The figure shows that for small to moderate particle size ranges, the numerical results are in excellent agreement with the analytical results even for the coarsest size grid. At large particle sizes, where number densities are small, the numerical results are overpredicted for a coarse grid. The figure, however, shows that by using a finer grid, the variation of number density even in this size range is predicted very well. This is clearly shown by the very good agreement across many orders of magnitude for $s = 1.25$, both for low and high degrees of aggregation. It should be pointed out that for $s = 1.5$ (a moderate grid), the extent of overprediction is much smaller than that for $s = 2$, and for applications requiring accurate information only in the densely populated size ranges, such a grid may provide acceptable accuracy. Of course for higher accuracy, a finer grid can always be used just by reducing the value of the s parameter. It is interesting to note that in comparison with pure breakup (for $s = 4$), the present example requires much finer grids ($s = 1.25$) to yield comparable accuracies. This issue is explored in detail in Section 4.4.

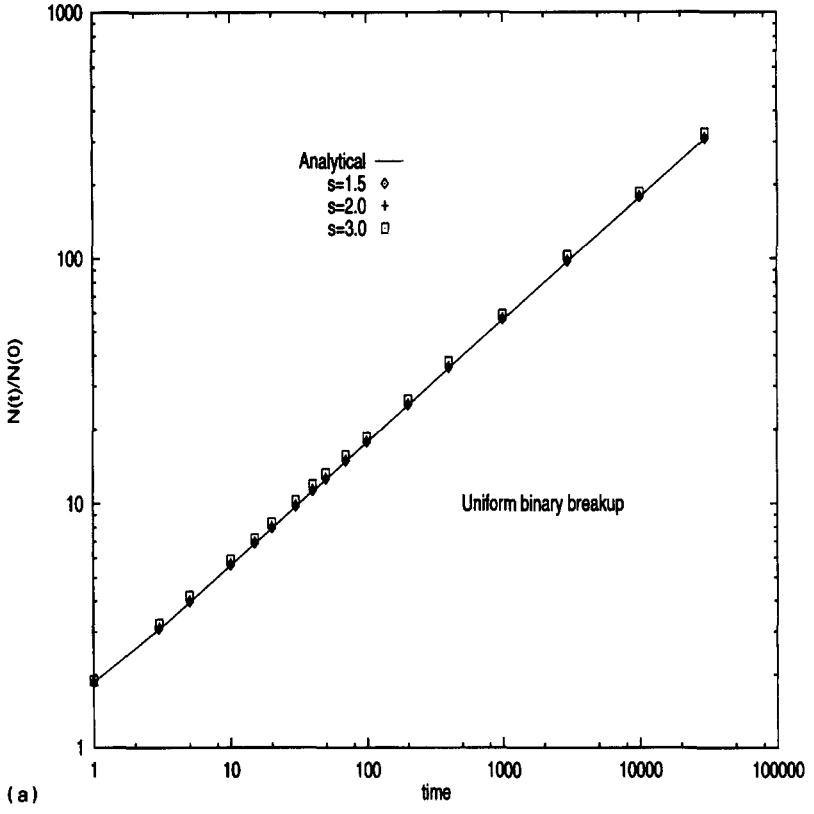

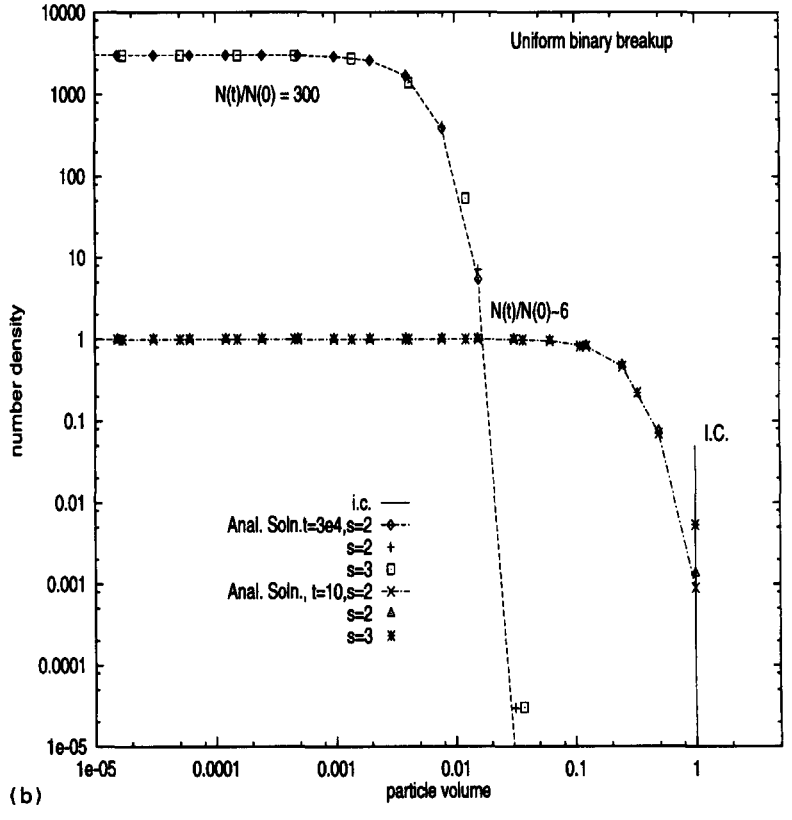

Fig. 3. (a) A comparison of the numerical and the analytical results (Ziff and McGrady, 1985) for the variation of total number of particles for *binary* breakage and $\Gamma(v) = v^2$. (b) A comparison of the numerical and the analytical size distributions for the case presented in Fig. 3(a).

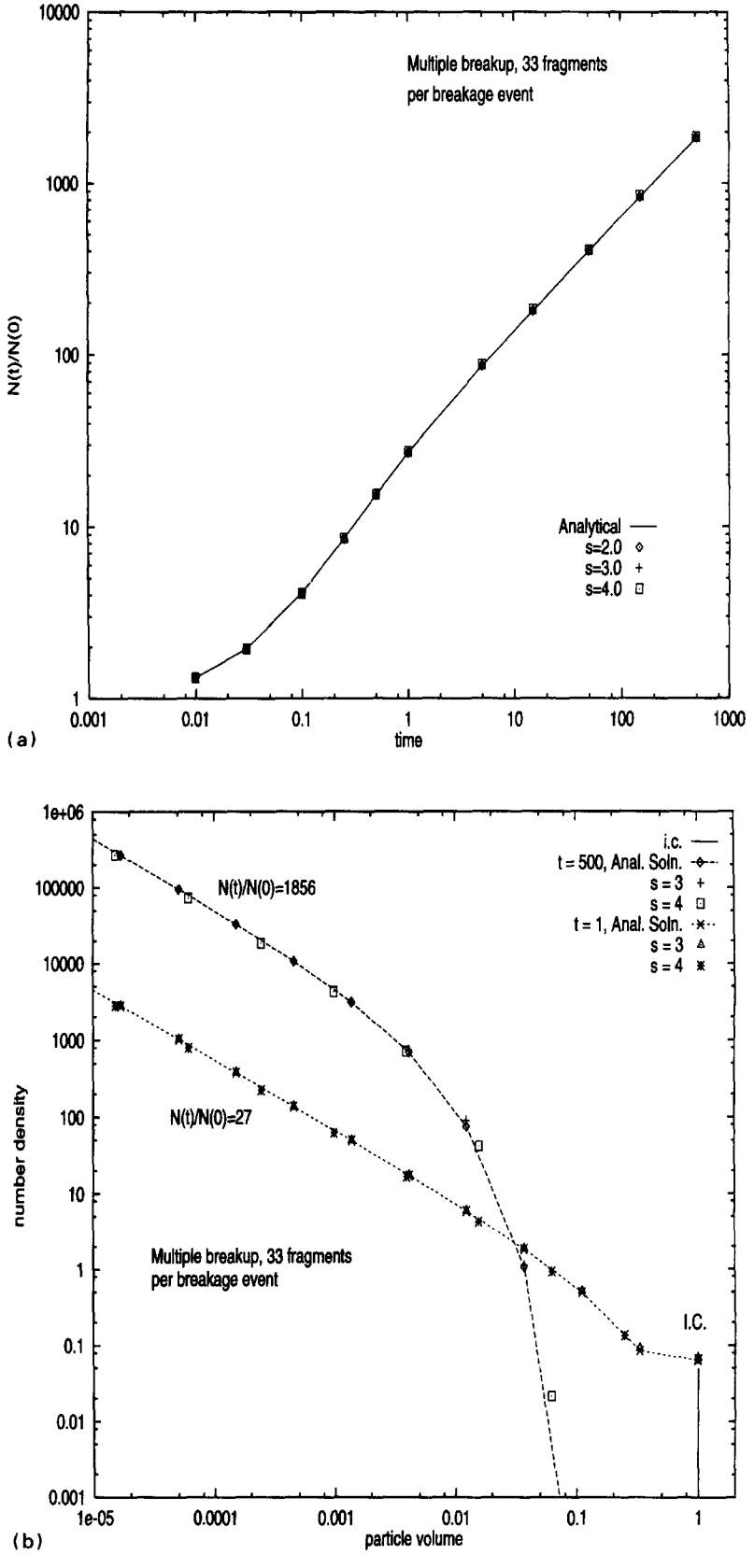

Fig. 4. A comparison of the numerical and analytical results (Ziff, 1991). (a) Variation of the total number of particles for *multiple* breakage of particles, $\Gamma(v) = v^{1.5}$. (b) Comparison of numerical and analytical size distributions for the case presented in (a).

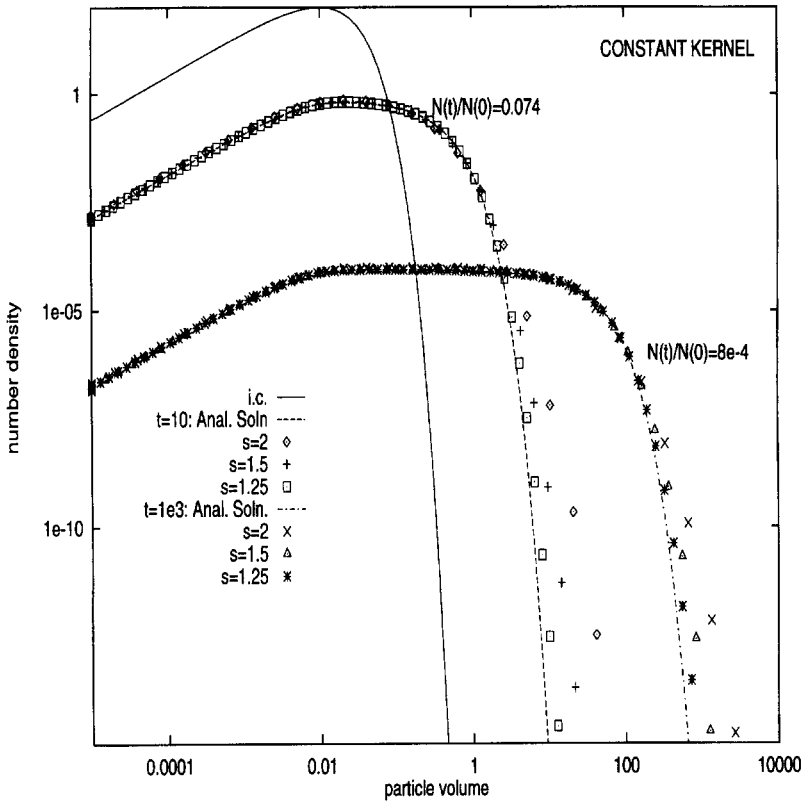

Fig. 5. A comparison of the numerical and the analytical size distributions (Scott, 1968) for pure aggregation with *constant* kernel, $Q(v, v') = \text{constant}$.

Figure 6 shows a similar comparison for the size-dependent sum kernel, $Q(x, y) = x + y$, for three values of parameter s (2, 1.5 and 1.15). Once again the same features are seen. The agreement at small sizes is very good for all three values of s. For $s = 2$, the numerical results for moderate size particles are underpredicted, and those for large sizes are significantly overpredicted. The use of finer grids ($s = 1.5$ and 1.15), as the figure shows, improves the accuracy significantly in the moderate as well as the large size range. Although the sum and the constant kernels have similar features, there is one important difference. The extent of overprediction for the sum kernel in the large size range is significantly larger [at $N(t)/N(0) = 0.039$ itself] than that for the constant kernel [at $N(t)/N(0)$ as low as 8×10^{-4}] and increases with time.

The results for a gelling-type kernel, $Q(x, y) = xy$, have been presented in Fig. 7 for the same values of parameter s as in Fig. 6. Like previous kernels, the agreement is good at small particle sizes for all grid selections, although for this kernel there is not much change in population in this size range. At moderate sizes, the coarse grid ($s = 2$) results in slight underprediction which is easily improved by selecting a smaller grid ($s = 1.5$). For large sizes, however, the coarse grid produces results which are not even in qualitative agreement with the analytical results even though the degree of aggregation is very low [$N(t)/N(0)$ being 0.925 and 0.75]. As the grid is made finer ($s = 1.15$), the predictions are improved significantly and the exponential tail is also predicted with improved accuracy.

The results presented in this section can be summarized in the following way. The number densities for smaller particles are predicted quite accurately even with a coarse grid. In general, maximum deviations are encountered in large particle size ranges where the number density decreases very steeply (exponentially). If the degree of homogeneity of the aggregation kernel is increased (zero for constant kernel, one for sum and two for product kernel), the deviations in this size range are increased, and as time progresses they continue to increase still further. The technique presented in this paper readily accommodates these issues by just reducing the grid parameter s which of course increases the computational costs. Although this option can be used to improve the accuracy of the numerical predictions to any desired degree, we shall address this issue again in Section 4.4 to explore more efficient ways of accomplishing it.

4.2.2. *Prediction of second moment of the distribution.* We now present some results to illustrate the usefulness of the concept of preservation of two

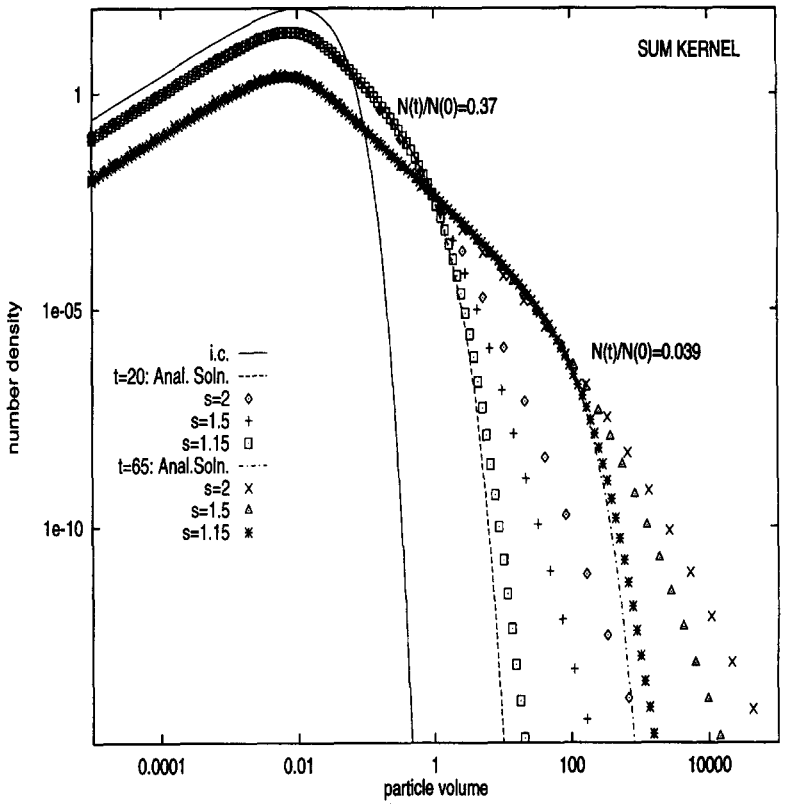

Fig. 6. A comparison of the numerical and the analytical size distributions (Scott, 1968) for pure aggregation with *sum* kernel, $Q(v,v') = v + v'$.

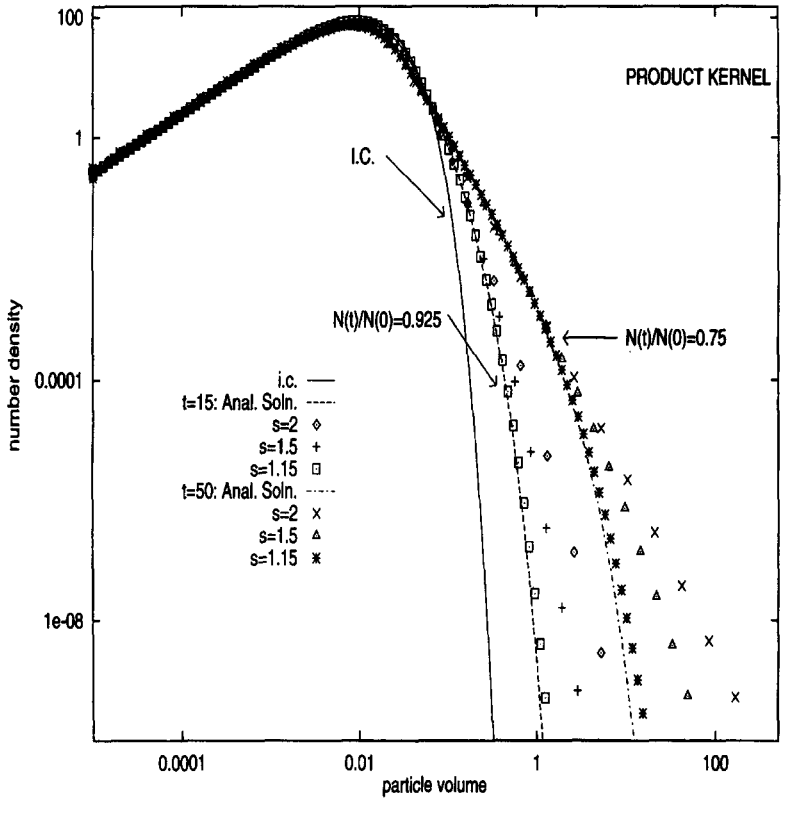

Fig. 7. A comparison of the numerical and the analytical size distributions (Scott, 1968) for pure aggregation with *product* kernel, $Q(v,v') = vv'$.

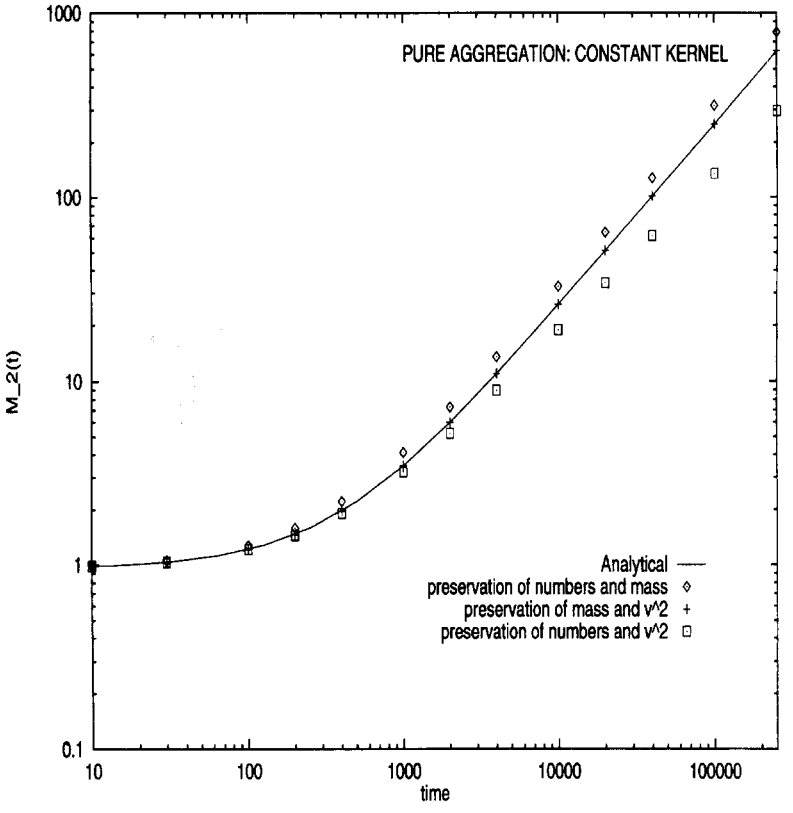

Fig. 8. The variation of the second moment of the size distribution with time for *constant* kernel: a comparison of numerical and analytical results.

appropriate properties in the set of discretized equations. We consider a simple case of pure aggregation and set the objective as prediction of variation of the second moment of the size distribution with time. From the applications viewpoint, the second moment of the distribution is proportional to the light scattered by particles in the Rayleigh limit. Figure 8 shows the results for the desired quantity for the constant kernel and three combinations of two properties that are preserved in the numerical technique: numbers and mass, mass and v^2, numbers and v^2. The results presented here have been obtained by using a coarse grid $s = 2$, and thus, when numbers and mass are preserved, they become the same as those obtained from the technique of Hounslow *et al.* (1988). A comparison of the numerical results (shown by points) with the analytical results (shown by solid line) indicates that the prediction of the second moment using a discretization technique that preserves numbers and mass yields poor results. The combinations involving the preservation of v^2 and numbers result in loss of mass from the system and, although the property v^2 is preserved, the results are of poorer quality than those obtained for the preservation of numbers and mass. The results obtained for the preservation of mass and v^2 are the best among the three combinations considered here, and are extremely accurate.

Very dramatic results are obtained for the size dependent sum kernel and are presented in Fig. 9. These results are obtained for the same coarse grid as mentioned earlier. The figure shows that the preservation of numbers and mass results in more than an order of magnitude overprediction for the second moment, and are of the worst quality for the three combinations considered here. Similarly, the preservation of numbers and property v^2 results in nearly an order of magnitude underprediction. In comparison, the results obtained by using the preservation of mass and property v^2, with the same coarse grid, $s = 2$, are once again extremely accurate.

A technique based on the preservation of fixed properties like numbers and mass (Hounslow *et al.*, 1988) can possibly predict such accurate results, but only with an extremely fine grid ($s = 1.05$), if allowed, incurring a much larger computational cost. These two examples clearly indicate that the flexibility of the present technique to conserve any two properties can be used to enormous advantage by making a correct choice for the properties that are preserved in the set of discrete equations. At this stage, it appears that mass conservation may always be imposed as a requirement for the discretized PBEs. However, further work is required to establish it unequivocally.

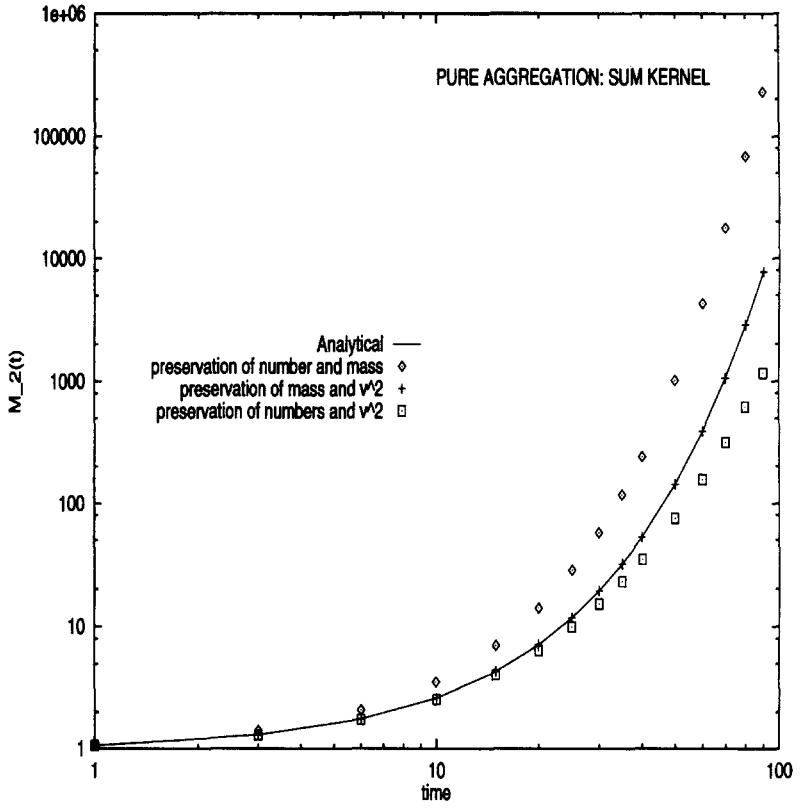

Fig. 9. The variation of the second moment of the size distribution with time for *sum* kernel: a comparison of numerical and analytical results.

4.3. *Simultaneous breakup and aggregation*

Blatz and Tobolsky (1945) have modeled the polymerization process by considering that the reaction of two small polymers leads to the formation of a large polymer and the breakage of a bond in a large polymer chain results in the formation of small polymers. Their final equation for the population of n-mers, based on these considerations, is given as

$$\frac{dN_k(t)}{dt} = \frac{k_f}{2}\sum_{1}^{k-1} N_i(t)N_{k-i}(t) - k_f N_k(t)\sum_{1}^{\infty} N_i(t) - k_b(k-1)N_k(t) + 2k_b\sum_{k+1}^{\infty} N_i(t). \quad (45)$$

For a monomer unit ($k = 1$), birth due to polymerization and death due to depolymerization are set equal to zero. The authors have provided an analytical solution for the set of equations (45) for an initial population of monomers. In the absence of an analytical solution (quite possible if the kernels are changed even slightly), one would need to solve a very large number of such equations (their numbers being equal to the degree of polymerization of the largest polymer, say 10,000) to arrive at the numerical solutions. In this section, we attempt to obtain a numerical solution for the population of monomers, dimers, trimers, etc. and also that of very large polymers by using as few as 40–50 equations. Let us proceed with the identification of the relevant kernels for this problem, which are given as

$$Q(v, v') = k_f, \quad \Gamma(v) = k_b(v-1), \qquad \beta(v, v') = \frac{2\delta(v - iv_*)}{(v'-1)}, \quad i = 1, 2, 3, \ldots \quad (46)$$

v_* is the volume of the monomer unit. Here $\beta(v, v')$ is the Dirac delta type function because the general equation [eq. (45)] is set in a strictly discrete framework. Since the populations of small polymers are of particular interest, we choose a special grid, such that $x_i = ix_0$ in the small size range and $x_{i+1} = sx_i$ for the large size range. In this particular example, we have used 15 uniform size sections to cover the discrete population of mono, di, tri, ..., 15-mers. The population of large polymers has been covered through a geometric grid.

The numerical results for such a grid, and for the preservation of properties $\zeta = 0$ and $\nu = 1$, are shown in Fig. 10. The lines show the analytical solutions at various times and the points represent the numerical solutions. The projection of all these points on the abscissa indicates the type of grid used here. The figure shows that the predictions of the transients as well as the steady-state distribution are extremely

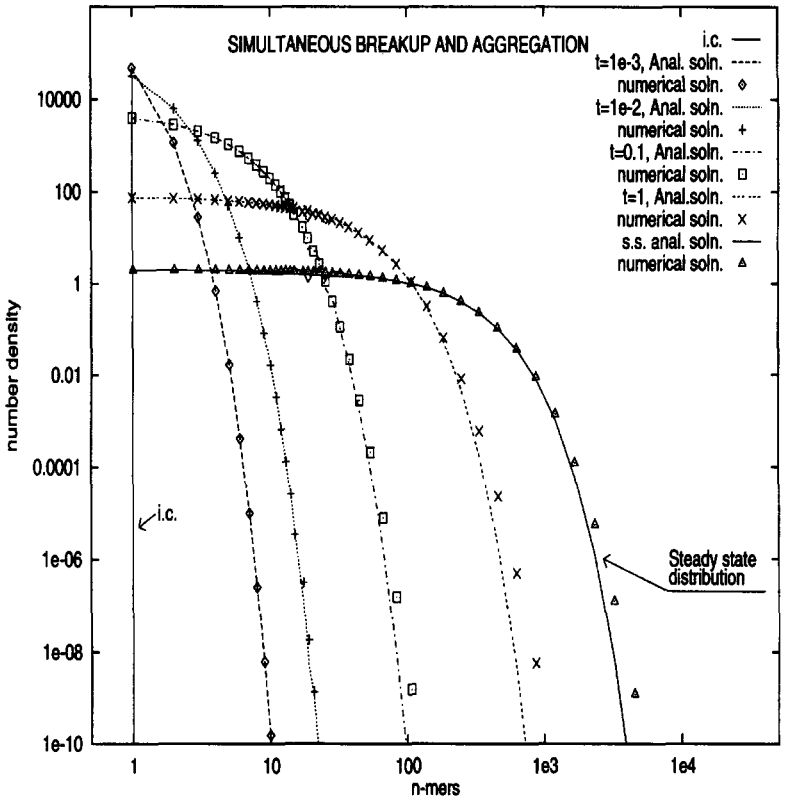

Fig. 10. A comparison of numerical and analytical size distributions (Blatz and Tobolsky, 1945) for the polymerization–depolymerization process (simulated as simultaneous breakup and aggregation). The projection of data points on the volume axis reveals the type of grid used here.

good. Although the kernels used here are discontinuous and difficult to handle, the numerical technique has correctly predicted the population of monomers, dimers, trimers, etc., and also that of large polymers. The issue of accuracy with small number densities in the large size range, pointed out earlier in Section 4.2.1, persists here too. The accuracy can, however, be improved by using a fine grid.

This example shows that the present technique successfully applies even to a very difficult example of simultaneous aggregation and breakup. The technique proposed here accomplishes this through its ability to extend itself to a general grid, adapted to suit a special situation — a uniform grid for small particles and a geometric grid for large particles. This example is also a good illustration of the applications of the discrete–continuous PBEs discussed earlier. The distribution of particles in these applications is such that, for small particle sizes, the continuum approximation breaks down, e.g. the population of monomers, dimers, etc. needs to be considered separately, and, for large particle sizes, the continuum approximation holds and an n-mer-type description can require 10,000's of discrete equations to be solved.

The present technique shows its ability to handle such situations very efficiently, offering enormous potential for solving problems associated with aerosol dynamics, polymerization and others where both fine resolution and long range are extremely important issues. The present technique also offers distinct advantages over the technique proposed by Landgrebe and Pratsinis (1990) [an extension of Gelbard *et al.* (1980)]. Their technique requires a large number of double integrals to be evaluated, and can preserve only one moment, which, as shown by Kostoglou and Karabelas (1994) for the technique proposed by Gelbard *et al.* (1980), does not yield good results for coarse discretization.

4.4. *Sources of error in numerical solutions*

In comparison with pure breakup, the numerical results for pure aggregation are found to be in error with the corresponding analytical solutions. The size distributions for the latter are consistently overpredicted in the size range where number densities decrease steeply. As aggregation proceeds, the extent of relative overprediction increases and the size range in which overprediction occurs continues to shift to new populations as they are born (in large particle size range). This feature is also common to the techniques proposed by Bleck *et al.* (1970), Gelbard *et al.* (1980) and Hounslow *et al.* (1988).

The inaccuracies in the numerical solutions have been considered to be due to the errors associated

with the discretization (similar to those associated with the evaluation of an integral by trapezoidal rule), and therefore the general strategy to improve the results is to use small discrete size ranges (equivalent to a small step size in integration) (Bleck, 1970; Landgrebe and Pratsinis, 1990). Although such a strategy definitely improves the numerical results, Figs 5–7 point out that the errors for coarse discretization are mostly confined to the size range in which the number density falls very steeply. We shall call the steep variation in number density as a front, and as can be seen from these figures the overprediction in this size range is because the front moves to larger sizes at a faster rate than its actual rate. In the rest of this section, we will investigate the reasons for this discrepancy. We hope that it will then suggest new ways of improving the accuracy of the numerical results.

We begin with a simple example of aggregation of particles in a size range $\{v_i, 2v_i\}$ with each other. Let us assume that the number density of particles in this size range is given as $n(v) = 1/v_0 \exp(-v/v_0)$, where v_0 is a parameter. For $v_0 \gg v_i$, the number density in the size range considered here is nearly uniform, and for v_i of the order v_0 or more it decreases exponentially. We now assume that the particles in this size range aggregate randomly (constant kernel). The number density of new particles, all of which lie in size range $\{2v_i, 4v_i\}$, can be calculated analytically, and has been plotted in Figs 11(a) and (b) for two values of parameter v_0, along with the number density of the aggregating particles.

Before we interpret these results, let us also consider the discretized version of the same event. The discrete version considers this process as the aggregation of N_i particles of size x_i, the representative size for size range $\{v_i, 2v_i\}$, to form $N_i/2$ particles of size x_{i+1} $(= 2x_i)$, the representative size for size range $\{2v_i, 4v_i\}$. A comparison of this representation with the actual process, as shown in Fig. 11(a) and (b), reveals that such a representation holds good only for uniform number density [Fig. 11(a)]. For exponential density, Fig. 11(b) shows that almost all the particles lie on the lower boundary of the size range, before as well as after the aggregation.

The discrete representation, on the other hand, advances the new $N_i/2$ particles to somewhere in the middle of the size range, resulting in an overprediction of the evolution. More importantly, if we had chosen a size dependent kernel, the discrete representation would have carried out the aggregation process at frequency $q(x_i, x_i)$, rather than a more relevant frequency that would correspond to the most populated size ranges. It is now clear that for size-dependent frequencies, the stronger the dependence of the frequency on its arguments, the larger the extent of overprediction. Our numerical results in Figs 5–7 clearly support this. As we go from constant to sum and product kernels, the degree of overprediction for the advancing front increases substantially.

The problems involving pure aggregation always accompany an exponential tail or an advancing front, even if the initial condition does not contain a front (van Dongen and Ernst, 1988). This indicates that the issue of overprediction will always be present with the discretized equations for pure aggregation, unless special efforts are made to prevent it. We propose two strategies to overcome this problem.

The first strategy is based on the use of the present technique with a variable grid. The second strategy involves a completely new technique that is sensitive to the variation of number density in a size range. The latter technique addresses large variations in number density across a size range by handling the cases presented in Fig. 11(a) and (b) differently and appropriately. In the present paper, we will confine ourselves to the first strategy. The second strategy involving the new technique has been presented elsewhere (Kumar and Ramkrishna, 1996).

5. SELECTIVE REFINING OF THE GRID

The previous section shows that a large variation in number density across a section width causes the front to move at a faster rate than its true rate. A simple strategy to correct it will therefore consist of choosing the section widths such that the number density does not vary significantly over a section width. This is easily accomplished through a nonregular grid (neither uniform nor geometric). The size range containing steep variation of number density is represented by a fine grid, and the rest of it is covered through a coarse grid.

The improvement brought about by this simple rearrangement of the grid points can be seen through a comparison of Figs 12(a) and (b). Figure 12(a) shows the numerical results for the sum kernel for $\zeta = 0$ and $\nu = 1$, obtained by using a regular geometric grid with 40 size ranges. Figure 12(b) shows the numerical result for the same case, but obtained by using a nonregular grid which has been selectively refined in the large size range and made coarse in the small size range (projection of all the points on abscissa indicates the type of grid used here). These figures reveal that a simple alteration in the grid type, while keeping the total number of sections the same, has improved the accuracy substantially without changing the computation time. It should be pointed out that this selection of nonregular grid is by no means the best possible. In fact, this is one of the most simple-minded alterations and a careful selection of the grid can further increase the accuracy. A similar improvement in the accuracy with a regular geometric grid requires the number of sections to be doubled, thus increasing the computation time approximately by a factor of eight.

As aggregation proceeds, the front (steep variation in number density) keeps advancing. Also, the population in the size range that initially contained the front evolves to contain relatively much less variation in number density. It would appear therefore that the computational effort can be further reduced by incorporating the mechanisms which, depending on the

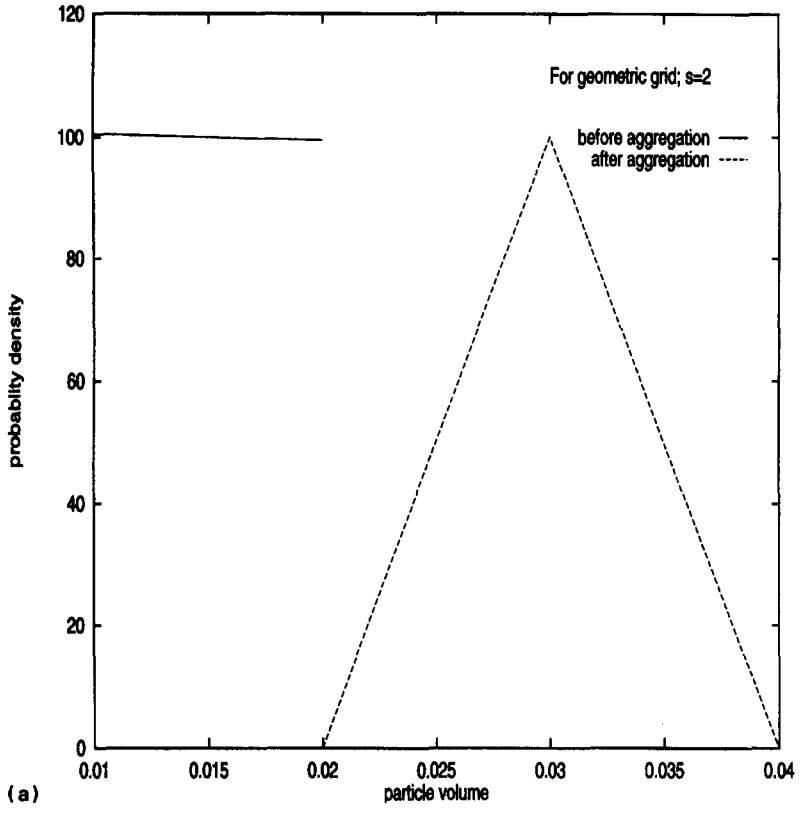

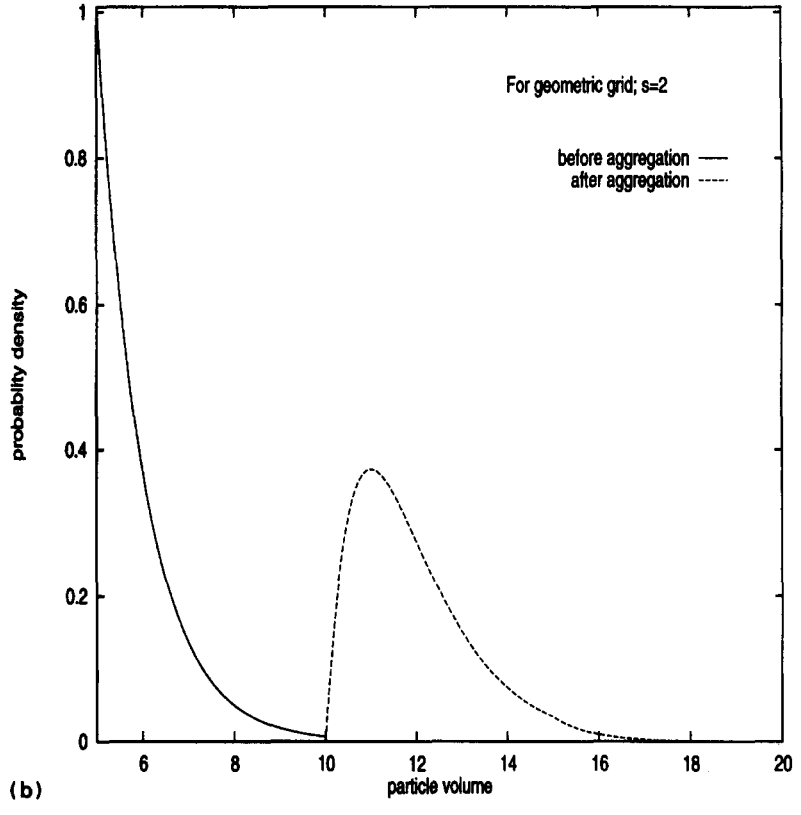

Fig. 11. Distributioon of particles before and after aggregation (constant kernel), when particles are initially distributed (a) *uniformly* and (b) *exponentially.*

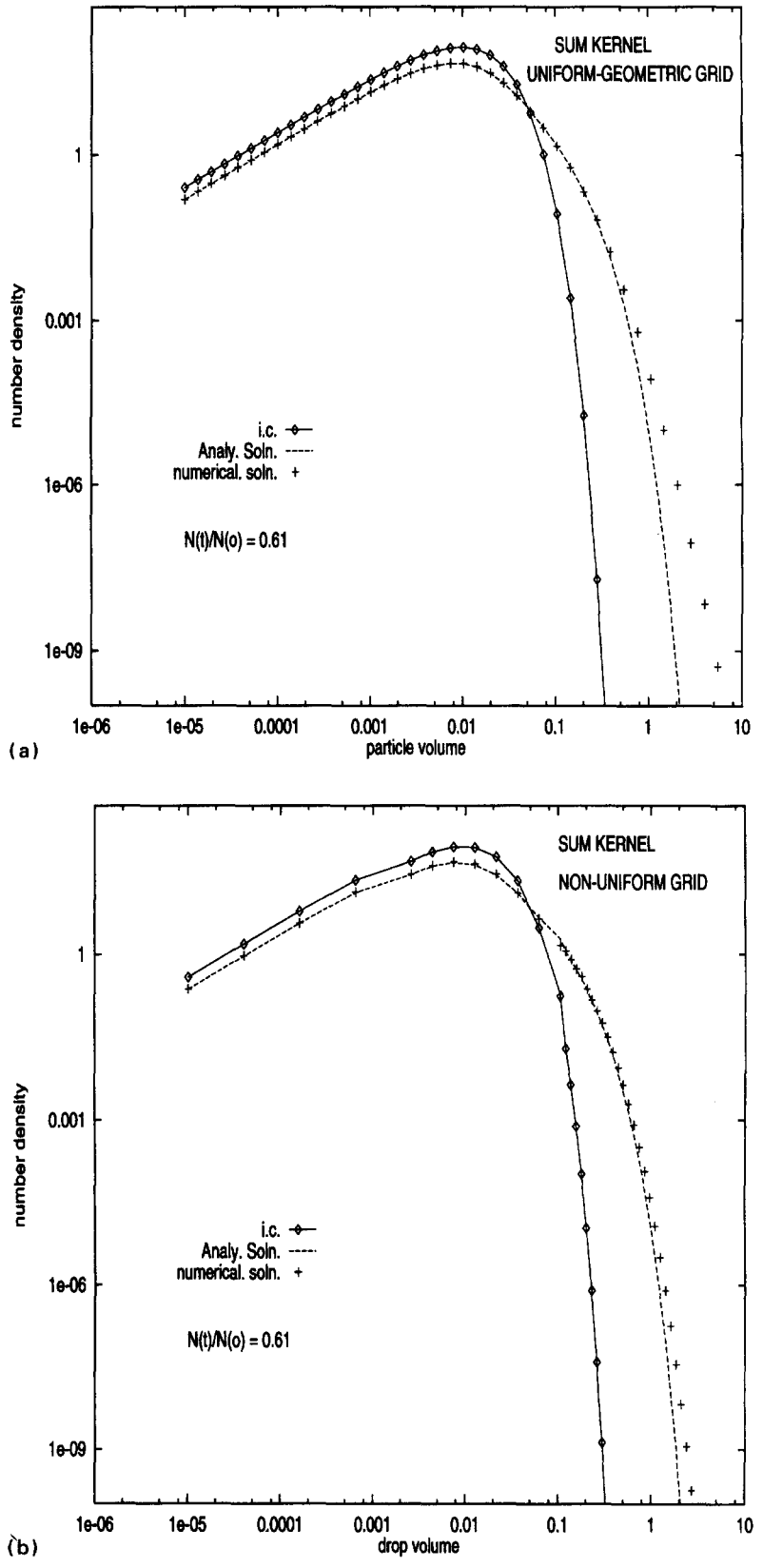

Fig. 12. A comparison of the numerical and the analytical size distributions (Scott, 1968) for pure aggregation with sum kernel, obtained by using (a) a *regular* geometric grid and (b) a *nonregular* grid. The projection of data points on the volume axis reveals the type of grid used.

variation of number density across a size range, change the pattern of the grid such that the propagation of error and the number of grid points are kept to a minimum. A fine grid, that no longer contains the front, can be changed to a coarse grid by assigning the populations at unwanted grid points to the neighboring grid points that are to be retained. This is analogous to how we have earlier dealt with the new particles that did not belong to any of the representative volumes. Thus, the fraction of the populations assigned to each neighbor can be obtained from eqs (21). Of course, the same properties that were preserved for the new particles will have to be preserved for these populations as well. As the front moves to large sizes, new fine sections, initially with zero population, are added to increase the size range covered in the computations.

These considerations may lead to the development of a very effective code that changes the grid automatically, adds a fine grid in the size range that contains the advancing front and changes the fine grid in the smaller size range to a coarse grid when a fine grid is no longer needed there. We are continuing with our efforts in this direction.

6. CONCLUSIONS

A new numerical technique to solve population balance equations has been presented here. It focuses on accurate prediction of the quantities of interest, while relaxing it for other less important quantities. The quantities of interest are determined by the requirements of the application, and can be either integral properties or the distribution of integral properties in terms of those for various size ranges. The discrete equations are designed to predict the desired quantities accurately through the simple idea that the representation of breakup or aggregation of particles should ensure exact preservation of the changes in the quantities of interest.

The proposed technique offers a general grid that can be effectively adapted to special situations including the ones that require a uniform grid in a certain size range and a nonuniform or geometric type grid elsewhere. Computationally, the technique presented here is very efficient as it does not require the evaluation of any double integrals.

The technique has been tested for pure binary and multiple breakup with power-law breakage rates and pure aggregation for the constant, sum and product kernels. In all cases, a comparison of the numerical and the analytical results shows that the agreement is very good. In comparison with pure breakup, the problems involving aggregation require a fine grid for comparable accuracies. This is because the number densities for the latter are overpredicted in the large particle size range.

The technique has also been tested for simultaneous breakup and aggregation for a difficult case of polymerization and depolymerization reactions. The numerical results obtained by using a combination of uniform and geometric grids show very good predictions right up to steady state. This example brings out the natural potential of the present technique to handle a whole new class of problems involving discrete–continuous PBEs in an efficient manner.

Most interestingly, numerical results for the prediction of second moment for the constant as well as the sum kernel show that a proper choice of the properties preserved in the set of discrete equations can result in substantial (more than an order of magnitude) improvement in the accuracy of the numerical solution. This work shows such an improvement for a fairly coarse grid.

Finally, it has been shown that the overprediction in the large size range is due to steeply varying density functions across a size range. The present work demonstrates that a selective refinement of the grid in the size range that contains steeply varying number densities and coarsening of the grid elsewhere can improve the accuracy of the numerical predictions for the same number of total discrete size ranges (same computation time). The concept of selectively refining the grid has been further developed to include a moving grid.

NOTATION

$a(v, x_k)$	number of particles of size x_k assigned when a particle of size v, such that $x_k \leqslant v \leqslant x_{k+1}$, is formed
$b(v, x_{k+1})$	number of particles of size x_{k+1} assigned when a particle of size v, such that $x_k \leqslant v \leqslant x_{k+1}$, is formed
$f(v), f_i(v)$	monotonically increasing functions of particle size v
$F(t), F_i(t)$	integral properties defined as $\int_0^\infty f(v)n(v, t)\,dv$, $\int_0^\infty f_i(v)n(v, t)\,dv$
k_b	a constant for breakage frequency $\Gamma(v) = k_b(v - v_0)$
k_f	aggregation frequency
M	total number of sections used to represent the total population
$M_\mu(t)$	μth moments of the size distribution at time t
$n(v, t)\,dv$	number of particles in size range v to $v + dv$, at time t
$\overline{n_i}(t)$	average number density of particles for the ith size range, at time t
$\langle n\rangle_i(t)$	mass average number density for the ith size range at time t, defined as $\int_{v_i}^{v_{i+1}} vn(v, t)\,dv / \int_{v_i}^{v_{i+1}} v\,dv$
$n_{i,k}$	total number of particles assigned to representative volume x_i, when a particle of size x_k breaks [given by eq. (27)]
$N(t)$	total number of particles at time t
$N_i(t)$	total number of particles in the ith size range at time t
$Q(v, v')$	aggregation frequency
$Q_{i,j}$	aggregation frequency for sizes x_i, x_j, $Q(x_i, x_j)$

R_{Ba}	birth term due to the aggregation of particles
R_{Bb}	birth term due to the breakage of particles
R_{Da}	death term due to the aggregation of particles
R_{Db}	death term due to the breakage of particles
s	a parameter that defines the geometric grid of the type $x_{i+1} = sx_i$
t	time
v, v'	particle volumes
v_i, v_{i+1}	lower and upper boundaries for the ith section
v_0	a parameter in eq. (44), equal to half the initial average volume
x_i	representative volume for the ith size range, also the ith grid point

Greek letters

$\beta(v, v')\,dv$	number of daughter particles formed in size range v to $v + dv$ due to the breakage of a particle of size v'
$\gamma(v)$	total number of daughter particles formed as a result of the breakage of a particle of size v
$\Gamma(v)$	breakage frequency for a particle of size v
Γ_k	defined as $\Gamma(x_k)$
η	defined by eq. (37)

REFERENCES

Batterham, R. J., Hall, J. S. and Barton, G., 1981, Pelletizing kinetics and simulation of full scale balling circuits, in *Proceedings of the 3rd International Symposium on Agglomeration*, Nurnberg, W. Germany, p. A136.

Blatz, P. J. and Tobolsky, A. V., 1945, Note on the kinetics of systems manifesting simultaneous polymerization-depolymerization phenomena. *J. phys. Chem.* **49**, 77–80.

Bleck, R., 1970, A fast, approximate method for integrating the stochastic coalescence equation. *J. Geophys. Res.* **75**, 5165–5171.

Chen, A. W., Fisher, R. R. and Berg, J. C., 1990, Simulation of particle size distribution in an aggregation–breakup process. *Chem. Engng Sci.* **45**, 3003–3006.

Gelbard F. and Seinfeld, J. H., 1979, The general dynamic equation for aerosols. *J. Colloid Interface Sci.* **68**, 363–382.

Gelbard, F., Tambour, Y. and Seinfeld, J. H., 1980, Sectional representation of simulating aerosol dynamics. *J. Colloid Interface Sci.* **76**, 541–556.

Hidy, G. M., 1965, On the theory of the coagulation of noninteracting particles in Brownian motion. *J. Colloid Interface Sci.* **20**, 123–144.

Hounslow, M. J., Ryall, R. L. and Marshall, V. R., 1988, A discretized population balance for nucleation, growth and aggregation. *A.I.Ch.E. J.* **34**, 1821–1832.

Koh, P. T. L., Andrews, J. R. G. and Uhlherr, P. H. T., 1987, Modeling shear flocculation by population balances. *Chem. Engng Sci.* **42**, 353–362.

Kostoglou M. and Karabelas, A. J., 1994, Evaluation of zero order methods for simulating particle coagulation. *J. Colloid Interface Sci.* **163**, 420–431.

Kumar, S. and Ramkrishna, D., 1996, On the solution of population balance equations by discretization–II. A moving pivot technique. *Chem. Engng Sci.* **51**, 1333–1342.

Landgrebe, J. D. and Pratsinis, S. E., 1990, A discrete sectional model for particulate production by gas phase chemical reaction and aerosol coagulation in the free molecular regime. *J. Colloid Interface Sci.* **139**, 63–86.

Marchal, P., David, R., Klein, J. P. and Villermaux, J., 1988, Crystallization and precipitation engineering—I. An efficient method for solving population balances in crystallization with agglomeration. *Chem. Engng Sci.* **43**, 63–86.

Nambiar, D. K. R., Kumar, R. and Gandhi, K. S., 1992, A new model for the breakage frequency of drops in turbulent stirred dispersions, *Chem. Engng Sci.* **47**, 2989–3002.

Narsimhan, G., Ramkrishna, D. and Gupta, J. P., 1980, Analysis of drop size distributions in lean liquid–liquid dispersions, *A.I.Ch.E. J.* **26**, 991–1000.

Ramkrishna, D., 1985, The status of population balances. *Rev. Chem. Engng* **3**, 49–95.

Sastry, K. V. S. and Gaschignard, P., 1981, Discretization procedure for the coalescence equation of particulate processes. *Ind. Engng Chem. Fundam.* **20**, 355–361.

Scott, W. T., 1968, Analytical studies in cloud droplet coalescence I. *J. Atmos. Sci.* **25**, 54–65.

van Dongen, P. G. J. and Ernst, M. H., 1988, Scaling solutions of Smoluchowski's coagulation equation. *J. Statist. Phys.* **50**, 295–329.

Ziff, R. M. and Mcgrady, E. D., 1985, The kinetics of cluster fragmentation and depolymerization. *J. Phys. A: Math. Gen.* **18**, 3027–3037.

Ziff, R. M., 1991, New solutions to the fragmentation equation. *J. Phys. A: Math. Gen.* **24**, 2821–2828.